Bitumen partial upgrading over Mo/ZSM-5 under methane environment: Methane participation investigation

Peng He, Lulu Zhao, Hua Song[*]

Department of Chemical and Petroleum Engineering, University of Calgary, 2500 University Dr. NW, Calgary, Alberta T2N 1N4, Canada

ARTICLE INFO

ABSTRACT

Bitumen extracted from oil sands which is abundant in Canada needs to be partially upgraded in order to meet pipeline specifications before being sent to downstream refineries. Hydrotreating where expensive hydrogen is involved at high pressure ($15 \sim 20$ MPa) is commonly employed as the technique to satisfy the upgrading requirement. In this study it is reported that a partially upgraded crude oil can be readily produced from bitumen under methane environment at mild conditions (400 °C and 3 MPa) without H_2 engagement under the facilitation of 5%Mo/ZSM-5 ($SiO_2/Al_2O_3 = 23:1$). The methane participation into the upgrading process was evidenced by analyzing the products obtained from the methanotreating of styrene and n-butylbenzene, the model compounds to represent heavy oil, as well as the heat effect during upgrading. Direct evidence of methane incorporation into the product molecules is observed on ^{1}H, ^{2}D and ^{13}C NMR spectra, revealing that the carbon and hydrogen from methane occupy the phenyl carbon sites and aromatic and benzylic hydrogen sites, respectively, in the product molecules. Through extensive catalyst characterizations using TEM, XRD, and XPS, the excellent catalytic upgrading performance might be closely related to the highly dispersed molybdenum oxide particles on the zeolite support at partially reduced oxidation state for better methane activation. The outcomes from this research could not only create an innovative route for more profitable natural gas utilization, but also benefit bitumen partial upgrading in a more economical and environmentally friendly way.

© 2016 Elsevier B.V. All rights reserved.

1. Introduction

The landscape of petroleum industry has been profoundly changed by the utilization of unconventional oils over the past decade, especially the past three years. The breakthroughs made in the extraction technology of shale oil is one of the forces that drive the crude oil price to be cut from above 100 USD per barrel in 2014 to below 30 USD per barrel in 2016. Another unconventional oil that is of large scale of potential reserve to serve as an alternative source of crude oil for suppling hydrocarbon chemicals and powering the world is heavy oil, such as bitumen extracted from Canadian oil sand, whose remaining proven reserves in Canada are 165 billion barrels by the end of 2015 according to the statistics released by Alberta Energy Regulator [1]. The heavy oil reservoirs are rich in several countries such as Canada and Venezuela, while the downstream refineries are mainly in other countries including United States. Unlike conventional petroleum deposit, heavy oil cannot be directly sent to existing refineries as the feedstock for fuels and lubricants production due to its high viscosity, high asphaltene content, low hydrogen to carbon ratio, and high impurities content [2]. For instance, the extracted bitumen from a typical Steam Assisted Gravity Drainage (SAGD) processes in Canada has an average density of 1.0077 g/cm^3, API gravity of 8.9, and a dynamic viscosity of 2×10^5–2×10^6 cP at atmospheric conditions [3]. Therefore, such heavy crude oil needs to be partially upgraded before transported to the downstream refineries through pipelines. Hydrogen thermal cracking (named hydrotreating) is widely practiced to break down the long carbon chain and especially the complicated polycyclic molecular structure of the high molecular weight residues, saturate the formed small molecules, and remove the impurities such as sulfur, nitrogen, and metal species from the partially upgraded crude oil simultaneously [4]. However, this process has to consume expensive and naturally unavailable hydrogen and operate at high pressure (e.g. $15 \sim 20$ MPa), resulting in a significant cost increase of this upgrading step. Therefore, it is critical to find out an alternative hydrogen donor which is readily available and abundant in nature and can be engaged at lower pressure for prominent upgrading cost reduction, making the whole process more economically attractive.

* Corresponding author.
E-mail address: sonh@ucalgary.ca (H. Song).

In industry, more than 50% hydrogen is obtained through steam reforming process of natural gas [5]. The reforming of methane is a highly endothermic reaction and often requires high operating temperature (>800 °C) and pressure (1.5–3.0 MPa) [6,7]. Instead of using hydrogen, if natural gas can be directly used as the reducing agent, the steam reforming process can be completely eliminated, leading to the cost reduction of the upgrading process. Moreover, compared to the traditional hydrotreating process, such novel process can produce extra synthetic crude oil originating from the incorporation of CH_4 into the carbon chain of cracked heavy crude oil. The increased product yield makes the upgrading process even more economically favorable. It is worth noting that in this scenario, rather than ejected as CO_2 to the environment by the steam reforming of natural gas, the carbon atoms of CH_4 remain in the product, thus reducing the greenhouse gas emission of oil industry and benefiting the environmental protection.

Natural gas, including its recently largely discovered form (shale gas), is another abundant natural resource present in North America. Due to its chemical inertness and low volumetric energy density, and the difficulty in the liquefaction process and transportation, natural gas is currently limited to the heating systems rather than liquid fuels or chemical feedstocks. In 2015, the price of natural gas in US is averaged US $2.77 per million British thermal units (MBTU), while that of West Texas Intermediate (WTI) light sweet crude oil is averaged US $48.79 per barrel, which is equivalent to US $8.79 per MBTU [1]. The underestimated value of natural gas has driven intensive studies over the past decades by a great many researchers regarding the activation of methane, the principal component of natural gas, and its conversion into valuable chemicals or liquid fuels. The study reported here aims to develop a novel catalytic process named methanotreating where methane can be activated and utilized to partially upgrade bitumen.

Compared to hydrogen, methane is more inert due to the more stable molecular structure (tetrahedron), making it more challenging to get activated. The strong and localized C—H bond impedes the activation of methane [8]. In order to make the aforementioned methanotreating reactions take place at the similar or even less severe conditions (e.g. lower operation pressure) of traditional hydrotreating process, methane should be activated more efficiently to readily participate in the reaction. Therefore, a specially tailored catalyst system should be developed to make methane as active as hydrogen for participating into the heavy oil upgrading process. The C—H bond energy of methane is as high as 435 kJ/mol, which is the highest among all hydrocarbons. Therefore, the desired catalyst should be able to effectively lower down the energy barrier so that the methane activation could happen at less severe reaction conditions.

According to literature, many researchers have dedicated themselves to the field of methane activation under nonoxidative condition over the past more than thirty years and many catalyst systems have been reported [9–15], among which zeolite supported molybdenum catalyst demonstrates the most promising activity toward methane conversion to higher hydrocarbons [16]. Even though, less than 10% methane conversion is observed when the temperature is higher than 700 °C with major products in aromatics. The active catalytic center is believed to be the molybdenum carbide species such as Mo_2C [17]. Recent studied shows that the Mo might exist in the ZSM-5 framework in more complicated states, such as Mo_2C_x (x = 1,2,3,4,6) and Mo_4C_x (x = 2,4,6,8) nanoparticles [18]. The reaction temperature for the effective activation of methane, however, is higher than 700 °C, impeding the application of this catalyst in petroleum refineries [17,19,20].

Nevertheless, the research by Choudhary et al. [21] and a series of following publications [22–30] have report that the activation and conversion of methane can be significantly enhanced in the presence of higher hydrocarbons, particularly unsaturated hydrocarbons, at much lower temperature region (400∼600 °C) and atmospheric pressure. Such pioneer work inspires us and sets the ground for the proposed technology in this work. Based on the reported synergetic effect, the cracked shorter carbon chain species formed during the upgrading of bitumen should help the activation of methane and its following conversion under the facilitation of appropriate catalyst. The methane molecule will be cleaved into CH_x and H_{4-x} species, which can be used to saturate the unsaturated molecules and remove the sulphur, nitrogen and metal out from the cracked products under the facilitation of the developed catalyst. During this process, more synthetic oil will be produced through the incorporation of CH_x moiety. Therefore, theoretically speaking, the synergetic effect between heavy oil and natural gas during methanotreating process should take place when suitable catalyst system is charged, which has been experimentally evidenced by Ovalles et al. [31,32] although not prominent and authors' encouraging previous research [33] on heavy oil upgrading as well as the ongoing studies on bio-oil upgrading [34–36] under methane environment at bench scale.

In this study, Mo/ZSM-5 catalyst was synthesized using impregnation method. The catalytic performance on bitumen partial upgrading under methane environment was evaluated at 400 °C and 3 MPa. The formed crude synthetic oil was extensively analyzed for its quality control in terms of viscosity, acidity, density, water content, gasoline & diesel content, asphaltene content, heating value, stability, and elemental composition. N-butylbenzene and styrene were selected as the model compound to represent the component of heavy oil for the investigation on methane participation. NMR spectra of oil products are acquired to verify the incorporation of methane into the product molecules where $^{13}CH_4$ and CD_4 are selected as methane sources. The heat effect from the upgrading reaction is studied by DSC to further confirm the methane participation. In addition, versatile characterization techniques including TEM, XRD, XPS, and TGA were employed to study the relationship between the structure of the developed catalyst and its catalytic performance.

2. Experimental

2.1. Feedstock and chemicals

A Canadian bitumen was acquired from Syncrude Canada Ltd. and used as received without further treatment. Toluene with a purity of > 99.5 wt.% (provided by VWR International) was used to isolate any possible toluene-insoluble solids in bitumen and its upgraded product (i.e. possibly coke and catalyst). Heptane (anhydrous, 99%, Sigma-Aldrich) was exclusively employed to determine asphaltenes content of various oil samples. N-butylbenzene with a purity of ≥99% and styrene (99.9%) manufactured by Sigma-Aldrich were used as the bitumen model compound.

2.2. Catalyst synthesis

The ammonium ZSM-5 zeolite with SiO_2/Al_2O_3 = 23 and specific surface area of 425 $m^2\,g^{-1}$ was purchased from Alfa Aesar and calcined at 600 °C for 5 h in air to attain the H-type ZSM-5 for further use. The 5 wt.% Mo/HZSM-5 was prepared by incipient wetness impregnation of HZSM-5 with Ammonium molybdate tetrahydrate $((NH_4)_6Mo_7O_{24}\cdot4H_2O$, 99%, Alfa Aesar) aqueous solution, dried in the oven at 92 °C overnight, followed by being fired at 600 °C for 3 h in ambient air. The resultant catalyst was stored for use.

2.3. Catalytic performance test

After passing leak test, eighty grams of bitumen with 1 wt.% catalyst was loaded into a Parr autoclave of 300 mL capacity and was

pressurized to 30 bar with reactive gas (i.e., methane) or nitrogen after the air inside the reactor was purged out. A heating mantle was used to bring the reactor temperature first from room temperature to 130 °C. The temperature was then maintained at 130 °C for 30 min under mechanic agitation for dispersing catalyst well into the bitumen feedstock. The autoclave was then quickly heated up to 400 °C (i.e. reaction temperature) and kept at the reaction temperature for 20 mins while stirring. When the upgrading was to be terminated, the autoclave body was plunged into a cold water bath and the temperature could be lowered below 300 °C in less than 2 min. The bitumen model compound was also upgraded in a similar matter in a Parr® autoclave of 100 mL capacity using 8.0 g n-butylbenzene. CH_4-alone run was carried out without the introduction of bitumen or model compound. The catalyst was mixed with 10.0 g CS_2 (GC grade, EMD Chemicals) to extract the liquid product adsorbed on the catalyst for GC–MS analysis.

In order to provide a more direct evidence for proving methane participation into the upgrading process, reaction between butylbenzene/styrene and CH_4, $^{13}CH_4$ and CD_4 (99.9% ^{13}C and 99% ^2D, respectively, Cambridge Isotope Laboratories, Inc.) were also conducted in the aforementioned 100 mL Parr® reactor. 0.5 g catalyst was charged into the reactor with a glass vial carrying 0.1 g butylbenzene/styrene. The reactor was pressured to 3 atm by CH_4, $^{13}CH_4$ or CD_4 after the air was purged out by N_2 at 1 atmospheric pressure. The reactor temperature was then ramped up with a rate of 20 °C/min to the destination temperature (400 °C) and held for 60 mins. Upon the reaction completion, the reactor was allowed to cool down to room temperature before product collection. The formed liquid product embedded into the charged solid catalyst was extracted out using 10.0 g CS_2 (GC grade, EMD Chemicals) as solvent and internal standard for following NMR analysis.

2.4. Characterizations

The water content of liquid sample produced from each run was determined using Karl Fischer titration (Metrohm 870 Titrino Plus) through averaging the results collected from at least three independent measurements.

The total acid number (TAN) of liquid sample produced from each run was measured using a Metrohm 848 Titrino Plus through averaging the results collected from at least three independent measurements.

A gas displacement density analyzer (AccuPyc II 1340) manufactured by Micromeritics was employed to measure the density of liquid sample at 15.6 °C. The measurement temperature is accurately controlled through a PolyScience® LS 51 compact recirculating chiller fabricated by Cole-Palmer.

The gasoline and diesel fraction distillation was performed by using a home-made distillation apparatus at a temperature of 350 °C for atmospheric distillation and at a temperature of 217 °C when vacuum was applied at −860 mbar.

The compatibility & stability feature of the collected oil samples was analyzed by engaging a TriboAmix® spot tester designed by TRIBOMAR GmbH and following a testing procedure defined in ASTM D4740.

The heating value of the liquid product was determined by an oxygen bomb calorimeter (Parr 6100 Compensated Jacket Calorimeter). The measurement was carried out at room temperature.

The viscosity of oil sample was determined by employing a Viscolead One Series L viscometer fabricated by Fungilab at temperature of 25 °C controlled through an incorporated hot water circulating batch.

The CHNS analysis was carried out using Elemental Analyzer (Perkin Elmer 2400 Series) in order to determine the C, H, N, S compositions of the oil samples.

The coke yield was obtained by first dissolving oil product in toluene. The resulting solution was then filtered and the collected filter paper was put into Soxhlet extractor for extraction until the toluene solvent in extractor was colorless. The collected filter paper was then dried in an oven for 2 h at 100 °C and weighed for coke amount determination.

The asphaltene contents of various oil samples were determined according to ASTM standard D 6560-00. Briefly, small amount of the sample was mixed with heptane and the mixture was heated under reflux. The resultant precipitated asphaltenes, waxy substances, and inorganic material were collected on a filter paper. The waxy substances were then removed by washing with hot heptane in an extractor. After removal of the waxy substances, the asphaltenes were separated from the inorganic material by dissolution in hot toluene. The obtained extraction solvent underwent evaporation and the received asphaltenes were finally weighed for calculating asphaltenes percentage.

The TEM experiments were performed by using Philips Tecnai TF-20 TEM instrument operated at 200 kV. An X-ray analyzer for EDS is incorporated into the instrument for elemental analysis under STEM mode for improving image contrast between C and Ag phases. The sample was first dispersed in ethanol and supported on lacey-formvar carbon on a 200 mesh Cu grid before the TEM images were recorded.

The crystalline phase compositions of prepared catalysts were examined by X-ray diffraction on a Rigaku Multiflex diffractometer with Cu Kα irradiation at a voltage of 20 kV and current of 40 mA in the 2θ range of 5–50°.

X-ray Photoelectron Spectroscopy (XPS) analysis was performed using an AXIS His, 165 Spectrometer manufactured by Kratos Analytical with a monochromatized Al Kα X-ray source. 2.3 V voltage was chosen to make the charge balance. A stainless steel sample holder was used. Survey scans were performed to identify all the elements within the sample, followed by more detailed regional scans for Mo 3d, C 1s, and O 1 s orbitals in order to achieve the high resolution for these elements of interest. A controlled-atmosphere transfer chamber was used for transferring the sample to the XPS instrument without exposure to atmosphere.

The gas products formed from the upgrading reaction were analyzed by a four-channel micro-GC (490, Agilent). Upon the reaction completion, the reactor was allowed to cool down to room temperature before product collection. The gas product was first discharged to a 2.2 L cylinder, which was previously purged by N_2. The gas temperature and pressure (300 ~ 400 kPa) within the cylinder were then recorded before the gas product was analyzed by the connected micro-GC equipped with thermal conductivity detectors, which can precisely analyze H_2, O_2, N_2, CH_4, and CO in the first channel equipped with a 10 m molecular sieve 5A column; CO_2, C_2H_2, C_2H_4, and C_2H_6 in the second channel installed with a 10 m PPU column; and C_3—C_6 and $C_{3=}$—$C_{5=}$ in the third and fourth channels charged with a 10 m alumina column and a 8 m CP-Sil 5 CB column, respectively. Ar and He were the carrier gases for the first and other three channels, respectively. The composition of the gas products were used to calculate the moles of each species using ideal gas law. The moles of methane in the feedstock was calculated in a similar manner to determine the methane conversion.

The composition of the product oil was determined by the pre-calibrated Gas Chromatography-Mass Spectrometer (GC–MS: PerkinElmer GC Claus 680 and MS Clarus SQ 8T) equipped with a Paraffins-Olefins-Naphthenes-Aromatics (PONA) column (Agilent HP-PONA). The oven temperature of the GC was programmed to hold at 35 °C for 15 min, ramp to 70 °C at 1.5 °C/min, rise to 150 °C at 3 °C/min and hold for 30 min, then ramp to 250 °C at 3 °C/min and hold for 2 min.

The ^1H NMR experiments were conducted at 9.4 T ($\nu_0(^1H) = 400.1$ MHz) on a BRUKER AVANCE III 400 spectrom-

eter with a BBFO probe. ^{1}H NMR chemical shifts were referenced to CHCl$_3$ at 7.28 ppm. A spectral width of 12 kHz and a pulse delay of 2 s were used to acquire 64 scans per spectrum. The NMR samples in the tubes were prepared by mixing 0.3 mL sample with 0.3 mL CDCl$_3$.

The [2]D NMR experiments were conducted at 9.4 T (ν_0(^{1}H) = 61.4 MHz) on a BRUKER AVANCE III 400 spectrometer with a BBFO probe. A spectral width of 2.5 kHz and a pulse delay of 7 s were used to acquire 512 scans per spectrum.

The ^{13}C NMR experiments were conducted at 9.4 T (ν_0(^{13}C) = 100.6 MHz) on a BRUKER AVANCE III 400 spectrometer with a BBFO probe. ^{13}C NMR chemical shifts were referenced to CDCl$_3$ at 77.26 ppm. A spectral width of 26 kHz and a pulse delay of 2 s were used to acquire 17000 scans per spectrum. The NMR samples in the tubes were prepared by mixing 0.3 mL sample with 0.3 mL CDCl$_3$.

Thermographic Analysis (TGA) signal along with the simultaneously collected Differential Scanning Calorimetry (DSC) signal fulfilled with a simultaneous thermal analyzer (PerkinElmer STA 6000) were engaged to study the involved reaction features, which was accomplished through ramping the sample temperature to the destination temperature with a rate of 40 °C/min under 30 mL/min N$_2$ flow and a hold for 30 min under various gas environments (i.e., CH$_4$, N$_2$ + butylbenzene/styrene vapor or CH$_4$ + butylbenzene/styrene vapor).

3. Results and discussion

3.1. Catalytic performance of bitumen partial upgrading

As shown in Tables 1–4 , a synergetic effect between methane and bitumen is clearly demonstrated during partial upgrading process when Mo/ZSM-5 catalyst is engaged under methane environment, leading to the production of partially upgraded oil with highest quality in terms of lowest viscosity (379 cP at 25 °C), lowest density (0.9642 g/cm^3 at 15.6 °C and equivalent API gravity at 15.1), lowest acidity (0.02 mg KOH/g), highest heating value (41.5 MJ/kg), lowest asphaltene content (9.41 wt.%), highest gasoline & diesel contents (36.8 wt.%), and highest H/C atomic ratio (1.71) as well as the highest liquid yield (96.9 wt.%) and acceptable coke formation (0.66 wt.%), compared to a series of control runs, indicating the most efficient carbon chain breakage and rearrangement once catalytic methanotreating process is taking place. With an initial methane pressure of 3.0 MPa and Mo/ZSM-5 charged, bitumen's viscosity is remarkably reduced from a very high value of 848,080 cP to as low as 379 cP under the methane environment, which is approaching the oil pipeline transportation requirement set by the governments of Canada and USA [37]. More importantly, it is worth noting that this notable viscosity reduction is accompanied by the highest liquid yield and acceptable coke formation when both Mo/ZSM-5 and methane at 3.0 MPa were engaged (Table 1). Higher liquid yield is observed whenever methane is present as evidenced in Table 1, which is especially true when Mo/ZSM-5 catalyst is charged, implying the incorporation of methane molecules into the partially upgraded oil product, particularly under the facilitation of specially tailored catalyst. Coke particles of over 1 wt% present in the partially upgraded crude oil may create deposition with time, which will probably result in clogging to endanger pipeline transportation. Therefore, at low-temperature (400 °C) and low-pressure yet relatively concentrated methane gas (3 MPa) can be effectively activated by Mo/ZSM-5 to partially upgrade viscous heavy oil for boosting flowability with fairly good stability and other properties, making pipeline transportation feasible of this unconventional petroleum resource and easing the downstream refining work.

3.1.1. Stability and compatibility of oil product

In order to gain a better picture of the stability and compatibility of the oil products collected from various runs as reported in Table 1 for securing its acceptable capability for long term storage and long distance transportation, the spot tests over all these oil samples were performed and the results are presented in Fig. 1. For the purpose of delivering a better illustration of the oil dispersion images included in Fig. 1, the reference spot description (Table S1 and Fig. S1) given by ASTM D4740 is also included. When this definition is referred, Fig. 1 clearly indicates that the oil product collected after bitumen partial upgrading under the environment of methane with Mo/ZSM-5 engaged exhibits the best stability and compatibility where the black inner ring completely disappears as evidenced in Fig. 1f and therefore can be considered as spot #1 according to the given reference, thus making it appropriate to be transported by pipeline with excellent stability.

3.1.2. Physical properties of oil product

Several additional properties of the oil samples reported in Table 1 are further analyzed and complied in Table 2 in order to better reflect the qualities of the partially upgraded oils. As one of the most important criteria for judging the bitumen upgrading degree, densities of all the aforementioned oil products are measured and included into Table 2 for comparison. The lowest density is easily witnessed over the oil sample collected under the methane environment with Mo/ZSM-5 charged, which is equivalent to 15.1 at API density and consistent with the viscosity reduction and gasoline & diesel fraction enhancement data present in Table 3. Such density reduction might originate from the increased hydrogen content and decreased contents of sulfur and nitrogen in the partial upgraded oil as shown in Table 4 according to the density-composition relationship description given by M. Gray et al. [38].

Furthermore, Table 2 also reports the less acidity of the partially upgraded oil as evidenced by the reduced TAN value which makes it less corrosive to the inner wall of the container, thus benefiting its long distance transportation and long term storage. As clearly indicated by the data shown in Table 2, the oil product acquired from methane run with Mo/ZSM-5 engaged demonstrates the lowest acidity (0.02 mg KOH/g), which is more than 100 times smaller than that of the raw bitumen and over 10 times smaller compared to those collected from its N$_2$ counterparts as well as that obtained from methane run without catalyst addition, clearly indicating the synergetic effect between bitumen and methane when suitable catalyst is charged.

As also shown in Table 2, the increased water content is accompanied by the reduced total acid number when partial

Table 1
Performance of bitumen upgrading under various environments at 3.0 MPa and 400 °C for 20 min.

Trial	Atmosphere	Coke yield (wt.%)	Liquid yield (wt.%)	Viscosity (cP at 25 °C)
Bitumen	–	–	–	848,080
–	N$_2$	0.31	94.9	1884
–	CH$_4$	0.25	96.0	1735
HZSM-5	CH$_4$	0.87	91.5	1664
Mo/ZSM-5	N$_2$	0.68	92.3	509
Mo/ZSM-5	CH$_4$	0.66	96.9	379

Table 2
Properties of the oil samples collected before and after bitumen upgrading under various environments at 3.0 MPa and 400 °C for 20 min.

| Oil Sample	Liquid Product Properties				
	Density (g/cm³)	TAN (mg KOH/g)	Water Content (wt.%)	Heating Value (MJ/kg)	Asphaltene content (wt.%)
Bitumen	1.0275	2.69	0.159	40.2	22.04
N_2	0.9964	0.54	0.146	39.4	16.81
CH_4	0.9892	0.23	0.163	40.9	16.15
CH_4 + HZSM5	0.9774	0.25	0.172	40.8	14.70
N_2 + Mo/ZSM5	0.9763	0.53	0.128	40.1	11.39
CH_4 + Mo/ZSM5	0.9642	0.02	0.206	41.5	9.41

Table 3
Gasoline and diesel fractions of the oil samples collected before and after bitumen upgrading under various environments at 3.0 MPa and 400 °C for 20 min.

Trial	Atmosphere	Gasoline (wt.%)[a]	Diesel (wt.%)[a]	Total gasoline and diesel (wt.%)[a]
Bitumen	–	0.3	11.8	12.1
–	N_2	6.5	20.2	26.7
–	CH_4	6.2	23.1	29.4
HZSM-5	CH_4	6.9	24.8	31.7
Mo/ZSM-5	N_2	6.1	25.0	31.1
Mo/ZSM-5	CH_4	12.7	24.1	36.8

[a] Uncertainties of gasoline, diesel and total fraction are 0.1, 0.1 and 0.2, respectively.

Table 4
Elemental analysis of oil samples collected before and after bitumen upgrading under various environments at 3.0 MPa and 400 °C for 20 min.

Oil Sample	Carbon (wt.%)	Hydrogen (wt.%)	H/C Atomic Ratio	Nitrogen (wt.%)	Sulfur (wt.%)
Bitumen	83.09	10.24	1.48	1.85	4.48
N_2	83.96	10.45	1.49	1.73	3.58
CH_4	84.14	10.57	1.51	0.95	4.05
CH_4 + ZSM-5	84.23	10.19	1.45	1.64	3.74
N_2 + Mo/ZSM-5	83.69	10.81	1.55	1.06	3.90
CH_4 + Mo/ZSM-5	83.31	11.87	1.71	1.01	3.37
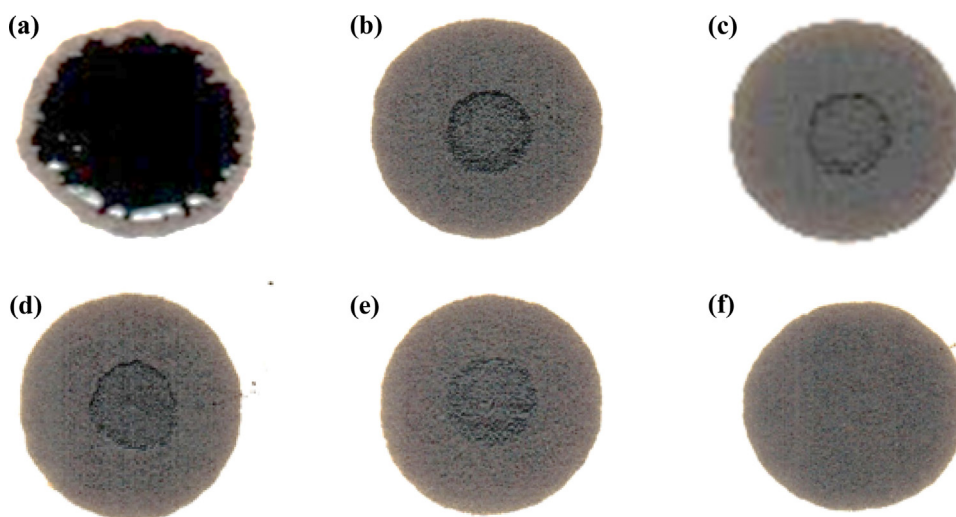
Fig. 1. Stability test of (a) bitumen and oil products collected under (b) N_2, (c) CH_4, (d) CH_4 with ZSM-5, (e) N_2 with catalyst Mo/ZSM-5, and (f) CH_4 with catalyst Mo/ZSM-5.

upgrading occurs under methane environment, particularly with the facilitation of Mo/ZSM-5 catalyst where highest water content (0.206 wt.%) is reached with the lowest TAN value at 0.02 mg KOH/g, which is probably due to the hydrodeoxygenation reactions taking place between oxygen containing molecules (e.g. hydroxyl and carboxyl groups) in cracked bitumen and hydrogen formed from activated methane [33].

The excellent upgrading capability of Mo/ZSM-5 during bitumen partial upgrading is further evidenced when the heating values of various oil products tabulated in Table 2 are compared. The methane runs always yield oil products with higher heating value when its N_2 counterparts are referred. The highest heating value

(41.5 MJ/kg) belongs to the oil product received during bitumen partial upgrading under methane environment when Mo/ZSM-5 catalyst is charged, thus providing another indirect evidence of methane incorporation into the molecules of the partially upgraded oil under the facilitation of suitable catalyst.

In order to evaluate the impact of catalytic methanotreating on the decomposition of asphaltene, the major contributor of the high viscosity of bitumen and the most difficult component in bitumen to be upgraded, the asphaltene contents of various oil products have been measured and the results are documented in Table 2. The oil product derived from catalytic methane run has the lowest asphaltene content (9.41 wt.%) and thus exhibits the highest asphaltene

reduction (∼57.3%) when the asphaltene content of raw bitumen is referred at 22.04 wt.%, further evidencing the positive contribution of the presence of Mo/ZSM-5 and methane as a combination to bitumen partial upgrading.

3.1.3. Compositional analysis of oil product

When a closer look is given to Table 3 for the gasoline & diesel fractions of the oil products reported in Table 1, it is worth noting that the gasoline fraction and the total gasoline and diesel fraction from bitumen partial upgrading in the presence of Mo/ZSM-5 under methane environment rank the highest among all the oil samples in comparison, which would definitely benefit its downstream refining at the other end of the pipeline and thus lead to significantly reduced production cost for its end use. Moreover, compared to those collected from all other control runs, the notable boost of gasoline fraction from catalytic methanotreating process provides us another evidence of the synergetic effect occurring between methane and bitumen during partial upgrading under the facilitation of suitable catalyst on bitumen molecules cracking and rearrangement for getting desirable final oil products.

In addition, elemental analyses of the oil products collected from various runs have also been performed and the results are presented in Table 4 for determining its saturation degrees in term of H/C atomic ratio and verifying the participation of methane into partial upgrading process. The highest H/C atomic ratio (1.71) is observed over the oil sample obtained from catalytic methane run, clearly confirming the involvement of methane and its positive role played on oil quality enhancement from raw bitumen with H/C atomic ratio of 1.48. Moreover, the increase of H/C atomic ratio is also accompanied by slight reduction of nitrogen and sulfur contents when referring to the raw bitumen's composition, implying the denitrogenation and desulfurization reactions happening to a small degree during bitumen partial upgrading.

In a brief summary, when Mo/ZSM-5 is charged under methane environment during the bitumen partial upgrading, the oil qualities get improved in the aforementioned aspects. Although such oil quality improvement may not meet all the industrial application criteria at the current stage for its end use, these obtained experimental results are valuable for revealing the role played by methane during the upgrading reaction, which would benefit the catalyst development in the future. In order to further probe how methane gets involved in the partial upgrading process, the mechanistic study is thus carried out through employing bitumen model compounds.

3.2. Mechanistic studies

3.2.1. Product distribution

It is widely accepted that bitumen has complex chemical composition and complicated molecular structure [39] and thereby a variety of its model compounds are frequently employed to trace upgrading chemistry. According to the literature [40,41], n-butylbenzene has both aromatic ring and saturated alkyl structure while remaining relatively simple in its molecular composition compared to other available candidates and is therefore used to represent bitumen in this research for studying the partial upgrading mechanism in the presence of activated methane. Compared to straight carbon chain paraffin or olefin with or without side chain, phenyl group containing ones would produce partially upgraded liquid product with much less variety in molecular structure since phenyl group is rather stable and difficult to undergo any structural change during partial upgrading. By substituting n-butylbenzene for bitumen in the liquid feedstock for the partial upgrading reaction, the reaction results are obtained and reported in Tables 5 and 6. There are no notable differences in final pressure, gas yield, liquid yield (Table 5) and liquid prod-

uct distribution (Table 6) when the gas environment is switched from N_2 to CH_4 without catalyst or support addition, and the same is true for conversions with addition of support yet in the presence of nitrogen or methane. N-butylbenzene overcracking in the presence of support is clearly shown in Table 5 by highest final pressure (6.0 MPa ∼ 6.1 MPa) coupled with highest gas yield (4.0 wt.% ∼ 4.1 wt.%) and lowest liquid yield (95.9 wt.% ∼ 96.0 wt.%) as well as in Table 6 by highest n-butylbenzene conversion (86.86% ∼ 87.66%) and liquid product formation with lower carbon number compared to those from its counterparts with catalyst charged. In addition, Table 5 also witnesses the lowest final pressure at 400 °C (4.6 MPa ∼ 4.7 MPa) from the runs in the absence of zeolite support or Mo/ZSM-5 where moderate gas yield is observed, indicating the least n-butylbenzene conversion. The lowest gas yields coupled with the highest liquid yields belong to the runs in the presence of Mo/ZSM-5 catalyst where the final pressures at the reaction temperature (i.e., 400 °C) are neither the highest nor the lowest, which is especially true for the catalytic methane run. When CH_4-alone run is carried out over Mo/ZSM-5, no gas or liquid products are detected, suggesting that these aforementioned phenomena are due to the synergetic effect between n-butylbenzene and CH_4 under the facilitation of the catalyst. A plausible explanation for this highly interesting phenomenon may be that for the conversions with Mo/ZSM-5, extra light hydrocarbons such as benzene were formed due to catalytic activation of methane; these light molecules can be gaseous at high temperature and liquid at room temperature. Furthermore, the lowest gas yield (3.1 wt.%) from the catalytic methane run which is even lower than that from the control run (3.7 wt.%) provides us more confidence in methane incorporation into the liquid product. The amount of gas products and their distribution formed from the n-butylbenzene upgrading over Mo/ZSM-5 under N_2 and CH_4 environment are displayed in Table S2. It is clearly observed that the moles of the gas products generated under CH_4 environment are larger compared to its N_2 counterpart, suggesting that some of the gas products are also derived from the conversion of methane.

In order to identify how methane gets involved in the upgrading process, the liquid products collected from various runs as shown in Table 5 are further analyzed by GC–MS and the major liquid product distributions as well as the conversions of n-butylbenzene and methane are summarized in Table 6. Benzene production is detected from all the reported runs. Moreover, it is worth noting that higher benzene formation is clearly observed whenever methane is present in the gas environment, implying the methane aromatization reaction might take place. However, this enhancement effect becomes diminished particularly when Mo modified ZSM-5 is charged, indicating that Mo might not be good at triggering methane self-aromatization reaction for benzene formation as what has been numerously reported by the researchers [16,17,21,25,42–46]. Nevertheless, the nonnegligible jump of methane conversion from 1.02% to 6.72% once Mo is introduced into the zeolite support might suggest that methane mainly gets involved into the reaction through adding its fragments formed from nonoxidative methane activation into the broken pieces originating from n-butylbenzene cracking under the facilitation of Mo loaded ZSM-5, which might lead to increased average carbon number of the produced aromatic products compared to that from its N_2 counterpart and thereby deserves further examination.

For further verifying the engagement of methane into the upgrading reaction, the major liquid products except for benzene collected over Mo/ZSM-5 and mainly listed in Table 6 under methane environment are compared to those collected from the run where N_2 is employed as the gas feedstock in term of its carbon distribution, the results of which are presented in Fig. 2. Toluene is the only product falling into the C_7 category. Ethyl benzene and xylene at trace amount are the products observed in C_8 group.

Table 5
Performance of *n*-butylbenzene upgrading under various environments at 3.0 MPa and 400 °C for 20 min.

Catalyst or support	Atmosphere	Final pressure (400 °C, MPa)	Gas yield (wt.%)	Liquid yield (wt.%)
–	N_2	4.7	3.6	96.4
–	CH_4	4.6	3.7	96.3
HZSM-5	N_2	6.0	4.1	95.9
HZSM-5	CH_4	6.1	4.0	96.0
Mo/ZSM-5	N_2	5.4	3.9	96.1
Mo/ZSM-5	CH_4	5.6	3.1	96.9

Table 6
Aromatics composition of liquid products and conversions of *n*-butylbenzene and methane at 3.0 MPa and 400 °C for 20 min.

Compound	Liquid Product Distribution/Conversion (wt%)					
	N_2	CH_4	ZSM-5, N_2	ZSM-5, CH_4	Mo/ZSM-5, N_2	Mo/ZSM-5, CH_4
Benzene	1.03	3.30	7.23	10.10	12.70	12.71
Toluene	25.14	22.84	0.88	1.16	9.56	1.13
Ethylbenzene	9.07	8.72	3.86	2.89	8.52	2.62
Styrene	14.58	12.29	0.06	0.16	–	–
Isopropylbenzene	–	–	6.62	6.56	6.27	7.93
N-propylbenzene	–	–	6.32	6.88	6.40	9.02
Methylpropylbenzene	2.71	1.61	7.14	6.97	6.32	8.04
Pentylbenzene	–	–	2.31	2.32	2.83	3.40
1,3,5-triethylbenzene	–	–	1.22	1.44	3.33	4.80
1,4-isopropylbenzene	–	–	0.47	0.52	6.28	7.32
1,4-dipropylbenzene	–	–	1.49	1.25	1.14	1.38
Hexylbenzene	–	–	0.84	0.78	0.97	1.00
1,1-diethylpropylbenzene	–	–	3.44	2.97	7.50	8.55
1,4-diisopropyl-2-methylbenzene	–	–	3.42	5.53	6.47	7.98
Propylpentylbenzene	–	–	0.70	0.60	3.27	3.35
1,3-(1-methylpropyl)-benzene	–	–	0.35	0.46	1.13	1.21
Butylbenzene[a]	10.70	10.90	86.86	87.66	80.83	75.30
Methane[a]	–	–	–	1.02	–	6.72

–: Below detection limit or not applicable.

[a] Conversion.
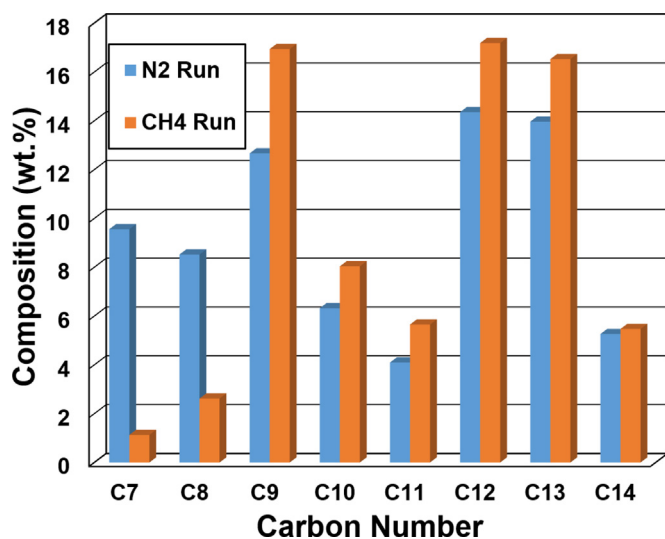
Fig. 2. The carbon number distribution in the liquid product collected over Mo/ZSM-5 at 400 °C and 3 MPa under CH_4 and H_2 environments.

C_9—C_{14} groups include the species with methyl, ethyl, propyl, butyl, pentyl groups, or their combinations attached to benzene as side chains. Fig. 2 witnesses the slightly lower liquid product formation with lower carbon number (C_7–C_8) followed by enhanced aromatics production with higher carbon number (C_9–C_{14}) when methane is present, indicating that methane might participate into the upgrading reaction and get incorporated into the molecular structure of the upgraded oil, thus leading to the shift of carbon number of the formed liquid product to the higher end when N_2 run is referred. Moreover, such aromatic products distribution analy-sis also evidences the increased average carbon number of these products from 7.85 (N_2 run) to 8.22 (CH_4 run), thus verifying the hypothesized reaction pathway for methane engagement during upgrading reaction.

3.2.2. NMR study of liquid products

The direct evidence of methane participation into the upgrading reaction is observed on the NMR spectra when isotope-labelled methane molecules are employed in the reaction with *n*-butylbenzene. Fig. 3 displays the ^{13}C NMR spectra of the products obtain when CH_4 and $^{13}CH_4$ are employed as the methane source to reaction with *n*-butylbenzene under the facilitation of Mo/ZSM-5 catalyst. The ^{13}C peaks in the ^{13}C NMR spectrum become much stronger from the $^{13}CH_4$ + butylbenzene run compared to that from its non-isotopic labelled counterpart, strongly indicating the methane involvement into the upgrading reaction. The peaks due to the phenyl carbon sites cannot be clearly observed in the NMR spectra of the oil product collected from the non-isotopic labelled CH_4 + *n*-butylbenzene run. When $^{13}CH_4$ is engaged in the reaction, six signals centered at 137.7, 129.1, 128.4, 128.0, 125.9 and 125.4 ppm are observed. The resonance at 137.7 ppm is assigned to phenyl carbon that is directly bonded to alkyl substituent groups. Its weak intensity, however, suggests that the concentration of ^{13}C at this position is not high. The peaks at 129.1, 128.4 and 128.0 ppm are attributed to the phenyl ring carbon atoms that are on the ortho and meta positions of the alkyl substituent, while the other two are due to the para carbon sites [47]. There are also a few weak peaks around 22 ppm and 30 ppm (not displayed), which might be due to alkyl group carbon sites, but the low peak intensity implies that the ^{13}C-enrichment are not strong at those sites. These observations indicate that during the reaction with *n*-butylbenzene, the carbon from CH_4 prefers the phenyl ring carbon sites, especially the ortho and meta positions. Furthermore, the non-uniform dis-
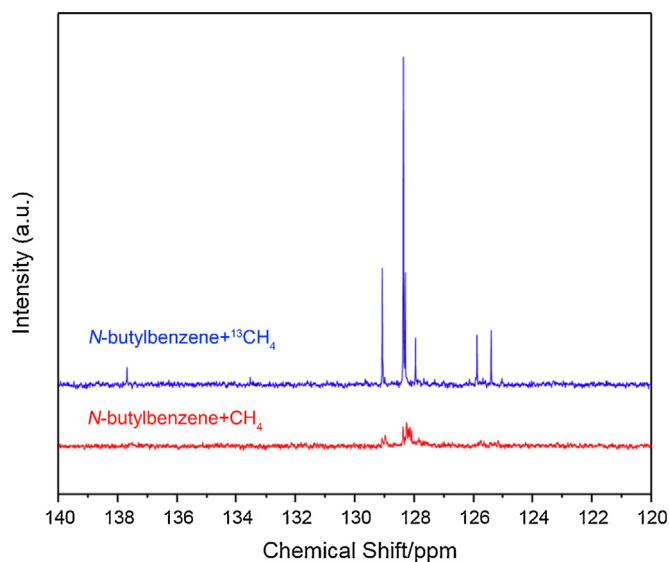
Fig. 3. The ^{13}C NMR spectra of the liquid products collected from the reaction between *n*-butylbenzene and $CH_4/^{13}CH_4$.
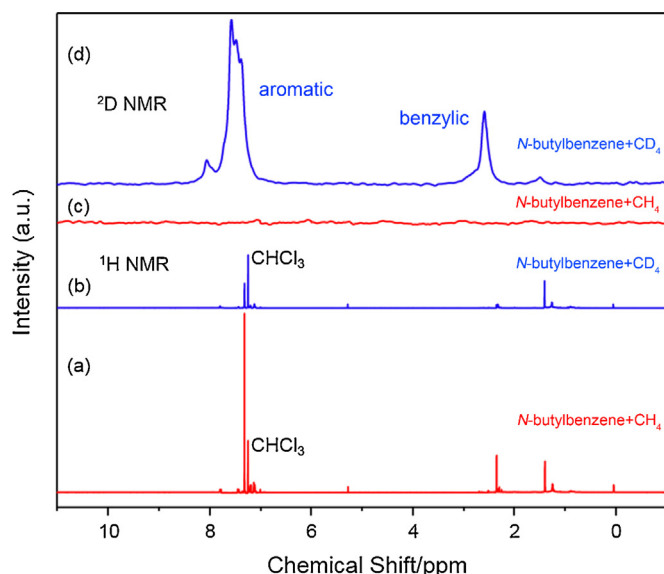

Fig. 4. The ^1H NMR spectra (a and b) and ^2D NMR spectra (c and d) of the liquid products collected from the reaction between *n*-butylbenzene and CH_4/CD_4.

tribution of ^{13}C signal at various carbon positions of benzene ring suggests that the broken pieces from *n*-butylbenzene cracking and activated methane might jointly provide the building blocks for benzene ring construction and subsequent aromatics formation.

Besides $^{13}CH_4$, deuterium-enriched methane, i.e., CD_4, is also used as the as the methane source to trace its pathway during the *n*-butylbenzene upgrading reaction. The ^1H and ^2D NMR spectra of the product (Fig. 4b and d) are acquired and compared with those of the non-isotopic enriched product (Fig. 4a and c) in order to probe the incorporation of the hydrogen atoms from methane to the products. On the ^1H NMR spectra, the peaks at 7.24 ppm are due to the $CHCl_3$ in the solvent, the intensities of which are similar in Fig. 4a and b. The intensities of other peaks, however, are suppressed significantly when CD_4 is present in the reaction. The peaks between 7.0 and 7.8 ppm are due to the H atoms on the phenyl rings. The signals between $2.0 \sim 2.7$ ppm can be assigned to benzylic H sites. Those appearing at the region below 2 ppm are attributed to H sites of the alkyl groups that are not bonded to phenyl rings directly.

Table 7
^1H NMR peak area ratio with respect to $CHCl_3$ of the products from *n*-butylbenzene and styrene upgrading under CH_4 and CD_4 environment.

H/D sites	*N*-butylbenzene			Styrene		
	CH_4	CD_4	Decrease/%	CH_4	CD_4	Decrease/%
Aromatics	7.4	3.3	56	4.2	1.0	76
Benzylic	2.8	1.0	64	1.1	0.13	89
Alkyl	4.9	4.9	0	3.8	3.6	5

The ratios between the peak areas with respect to that of $CHCl_3$ are shown in Table 7. The peak areas due to aromatics and benzylic H sites are greatly reduced in the isotopic labelled products, while the peak area due to H of alkyl groups remain unchanged, suggesting that the hydrogen from methane are enriched in the aromatic and benzylic sites over the alkyl group hydrogen sites. It is further confirmed by the ^2D NMR spectra, where the NMR signals of the D atoms are observed at the aromatic ($7 \sim 8$ ppm) and benzylic (2.5 ppm) sites.

In order to better understand the reaction mechanism, styrene, the primary liquid product from neat thermal cracking of *n*-butylbenzene as reported by Savage et al. [40,41], is also used as the feedstock to represent the bitumen molecules that react with methane during the upgrading reaction. Fig. S2 displays the ^{13}C NMR spectra of the products obtained when CH_4 and $^{13}CH_4$ are employed as the methane source to reaction with styrene under the facilitation of Mo/ZSM-5 catalyst. Similar phenomena are observed when the spectra obtained from *n*-butylbenzene upgrading are referred in Fig. 3. The ^{13}C peaks also become obviously observed in the NMR spectra acquired from $^{13}CH_4$ + styrene run compared to that from its non-isotopic labelled counterpart, clearly demonstrating the methane involvement into the product molecules. The peaks assigned to the phenyl ring carbon atoms that are on the ortho and meta positions, as well as those on the para carbon sites, are present on the spectrum. The peak due to the phenyl carbon that is directly bonded to alkyl substituent groups, however, is not detected. These observations indicate that during the reaction with styrene, the carbon from CH_4 prefers the phenyl ring carbon sites, especially the ortho and meta positions. Compared with the NMR spectra acquired from the upgrading of *n*-butylbenzene (Fig. 3), the ^{13}C-enrichment at the phenyl ring carbon position that is bonded to alkyl substituent is suppressed when styrene is employed as the liquid feedstock. Besides that, the ^{13}C distributions are similar in the upgrading products of *n*-butylbenzene and styrene, implying that styrene might be a key intermediate during the *n*-butylbenzene upgrading under methane environment.

In a similar matter, the ^1H and ^2D NMR spectra of the styrene upgrading product with CD_4 engaged as methane source (Fig. S3b and d) are also acquired and compared with those of the non-isotopic enriched product (Fig. S3a and c) in order to understand the incorporation of the hydrogen atoms from methane to the products. The peak intensity reduction at the aromatic and benzylic hydrogen regions on the ^1H NMR spectra (Fig. S3a and b) is also clearly observed and accompanied by the appearance of the ^2D NMR peaks (Fig. S3d) at the corresponding locations, demonstrating the incorporation of D atoms from methane into these sites during the reaction. Compared with what are observed from the *n*-butylbenzene upgrading, the ratios between the peak areas with respect to that of $CHCl_3$ are more significant as reported in Table 7, indicating that the incorporation of the hydrogen from methane into the products is more significant. The enhanced incorporation when *n*-butylbenzene is replaced by styrene as liquid feedstock further suggests that styrene might be a key intermediate formed during the *n*-butylbenzene upgrading under methane.

Based on the NMR study of the isotopic labelled and non-isotopic labelled products formed from model compound upgrading under
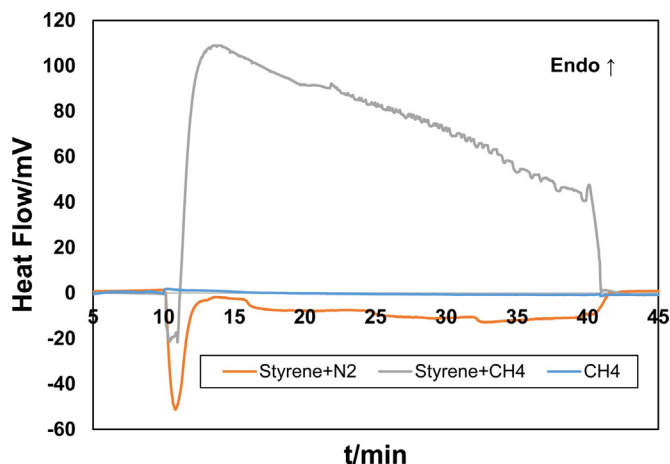
Fig. 5. The DSC profiles collected during the reaction of styrene over 5%Mo/ZSM-5 under various environments and methane-alone run at 400 °C and 1 atm.

Fig. 6. XRD patterns of ZSM-5 and Mo/ZSM-5 before and after *n*-butylbenzene upgrading at 3.0 MPa and 400 °C for 20 min.

methane environment, it can be concluded that a large fraction of hydrogen at the aromatic and benzylic positions of the product molecules is from methane during the reaction, while the carbon from methane favors the ortho and meta positions of the phenyl rings of the product molecules. Styrene might be a key intermediate formed during the *n*-butylbenzene upgrading under methane environment over Mo/ZSM-5 catalyst.

3.2.3. Reaction heat effect

The methane engagement into the styrene upgrading reaction with Mo/ZSM-5 charged is also investigated through employing DSC. The heat flow when the mixture of CH_4 + styrene is introduced at 400 °C (10 ~ 40 min) is displayed in Fig. 5. For better comparison, the results collected from its N_2 counterpart and the methane-alone run are also included. A stronger positive peak is clearly witnessed over styrene + methane run while that from its N_2 counterpart presents a weak negative feature, indicating more endothermic feature occurring from the interaction between methane and styrene molecules. The heat flow under CH_4 alone is also demonstrated in Fig. 5, which does not show strong endo- or exothermic effect due to its chemical inertness as discussed in the introduction part, suggesting that the dramatically changed heat effect is attributed to the synergetic effect occurring between styrene and methane molecules. In addition, the gradual decline in heat flow with increasing time is witnessed during the reaction between styrene and CH_4. This phenomenon can be attributed to the catalyst deactivation due to coke deposition. Due to the deficit of hydrogen in the styrene molecules, it should form polyaromatics such as naphthalene to balance the equation when forming other aromatics such as toluene, ethylbenzene and trimethylbenzene, which have higher H/C atomic ratios. Based on this assumption, thermodynamic calculations considering the conversion of styrene towards naphthalene, as well as a mixture of naphthalene with toluene, ethylbenzene and trimethylbenzene at 400 °C and 1 atm result in an enthalpy change of −18.7 ~ −11.2 kcal/mol-styrene. When methane participates in these reactions, the enthalpy changes are changed to −9.2 ~ 10.2 kcal/mol-styrene, demonstrating a much higher endothermic contribution. Therefore, such endothermic heat effect of the styrene + methane run may provide another evidence of methane participation into the upgrading reaction.

In a similar matter, the DSC measurement results of the *n*-butylbenzene upgrading with and without methane are demonstrated in Fig. S4. The exothermic feature observed in *n*-butylbenzene + N_2 run is suppressed in the *n*-butylbenzene + CH_4 run. Compared with styrene, a longer side chain is present in *n*-butylbenzene, which can be converted to more gas phase products.
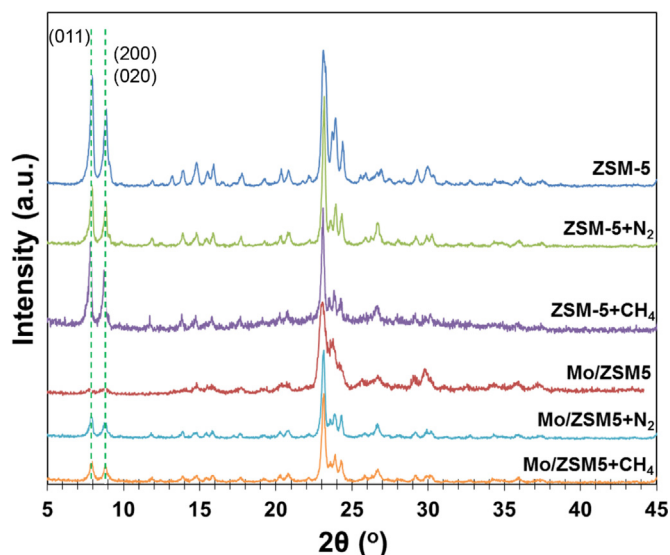
When methane is present, the carbon number of the liquid products tends to be increased, and the fraction of H_2 is also increased in the gas phase. The formation of more gas products such as hydrogen and ethane is confirmed by micro-GC analysis of the products obtained at 3 MPa. Based on these observations and assumptions, some thermodynamic calculations considering the conversion of *n*-butylbenzene towards naphthalene, ethylbenzene, propylbenzene, hydrogen, ethylene and ethane are carried out at 400 °C and 1 atm, resulting in an enthalpy change of −14.4 ~ −8.1 kJ/mol-butylbenzene. When methane is present, 1-methylnaphthalene and propylbenzene are used to replace naphthalene and ethylbenzene in the calculations, and the formation of H_2 is added to balance the equation, resulting in an enthalpy change of 2.3 ~ 25.2 kJ/mol-butylbenzene. Therefore, the participation of methane in the conversion of *n*-butylbenzene partially offsets its exothermic feature, which is observed in the DSC results.

3.3. Catalyst characterizations

3.3.1. XRD and TEM

For gaining a better understanding of the physical properties of the Mo/ZSM-5 catalyst system and its evolution during the upgrading of *n*-butylbenzene as well as its correlations with the catalytic upgrading performance, characterizations using XRD, TEM, and XPS have been performed and the collected results have been reported in Figs. 6–9 accordingly. From the comparison of the XRD patterns collected from ZSM-5 and Mo/ZSM-5 as shown in Fig. 6, it can be easily seen that the diffraction pattern of ZSM-5 majorly remains unchanged after active metal loading and during reaction, indicating that its framework is well maintained. In addition, the diffraction peaks of molybdenum oxide or metallic Mo are not detected, which is possibly due to its high dispersion. The peak around 8° is assigned to (011) plane, while the one around 9° is due to (200) and (020) planes. Upon the loading of the molybdenum on ZSM-5, the peak intensities are reduced significantly. A plausible explanation is that the doped Mo species might migrate into the HZSM-5 framework and reduce the crystalline of these planes. After the reaction, the Mo species may migrate away from these planes, resulting in an enhanced crystalline and thus increased peak intensities.

The morphology and particle size as well as elemental composition of fresh Mo/ZSM-5 are further investigated using TEM
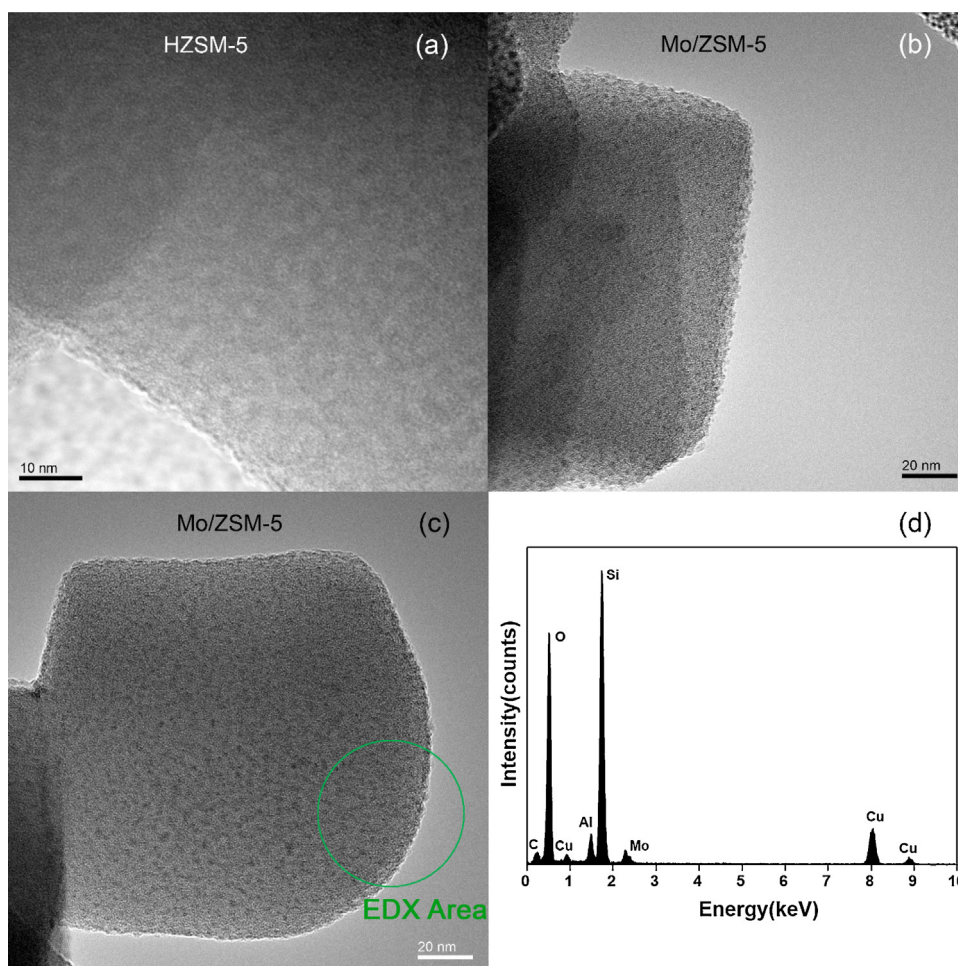
Fig. 7. TEM image of HZSM-5 (a), fresh Mo/ZSM-5 (b and c) and the corresponding EDX spectrum (d).

equipped with Energy-dispersive X-ray (EDX) spectroscopy. Fig. 7 shows the TEM image of one representative area of the catalyst and its associated EDX spectra after focusing on the circled particles spot. By combing the TEM image and EDX spectra, it can be concluded that the highly and uniformly dispersed particles shown as the black small dots in Fig. 7b and c, which are not observed on the fresh HZSM-5 images (Fig. 7a), are composed of molybdenum oxide with averaged particle size of 2 nm as evidenced by the corresponding EDX spectrum in Fig. 7d. The Cu peaks identified in this and following EDX spectra originate from the Cu grid used to support the catalyst particles during the TEM image acquisition rather than from the catalyst.

According to the TEM image of the catalyst collected before and after upgrading reaction (not shown), the channel structure of H-ZSM-5 were still kept even after the reactions at high temperature and high pressure (under N_2 or CH_4 conditions), which is consistent with the XRD results reported in Fig. 6. Nevertheless, as shown in Fig. 8a, the particle sizes (~4 nm at averaged value) of spent Mo/ZSM-5 catalyst collected under N_2 environment are slightly bigger than those of fresh one when Fig. 7b is referred, indicating light aggregations of loaded metal species after the reaction under N_2 condition. However, the size of the active metal particles is well maintained at 2 nm when CH_4 is present, as evidenced by Fig. 8c, which indicates that CH_4 condition is beneficial for the sintering prevention of loaded metal species and thereby makes positive contribution to the catalytic performance. In addition, the loaded active metal oxides also undergo partial reduction during the upgrading process, particularly under methane environment

as evidenced by the reduced oxygen intensity and its related intensity to that of the Si intensity from the comparisons between Figs. 7 d and 8 b and between Figs. 7 d and 8 d. The lower oxidation state of the active species achieved under methane environment might be also closely related to its better catalytic performance toward bitumen partial upgrading.

3.3.2. XPS

In order to get a better understanding of how each element contained in the Mo/ZSM-5 gets distributed on the catalyst surface and their corresponding oxidation state, XPS has been employed for conducting specific scans at Mo 3d, O 1s, and C 1s regions, respectively, and their results are disseminated in Fig. 9. As shown in Fig. 9a, Mo exists in the fresh catalyst as oxidation state of 6+ corresponding to the presence of MoO_3 after referring to its characteristic $3d_{5/2}$ binding energy at 232.6 eV. After reaction, the surface concentration of Mo gets reduced probably due to its diffusion into inner pores of the zeolite support, which is evidenced by the reduced peak intensities. Moreover, surface Mo gets partially reduced during reaction, as witnessed by the formation of additional shoulder peak with lower binding energy at 229.3 indicating the existence of Mo^{4+} according to the characteristic binding energy of MoO_2. Such observation is reasonable when the reducing reaction environment is taken under consideration. After a closer look at the two spectra collected after reaction, it is noticed that higher amount of Mo^{6+} and Mo^{4+} species as active phase is still present on the catalyst surface after the reaction under methane environment than that from N_2 run, which might be closely related to its better
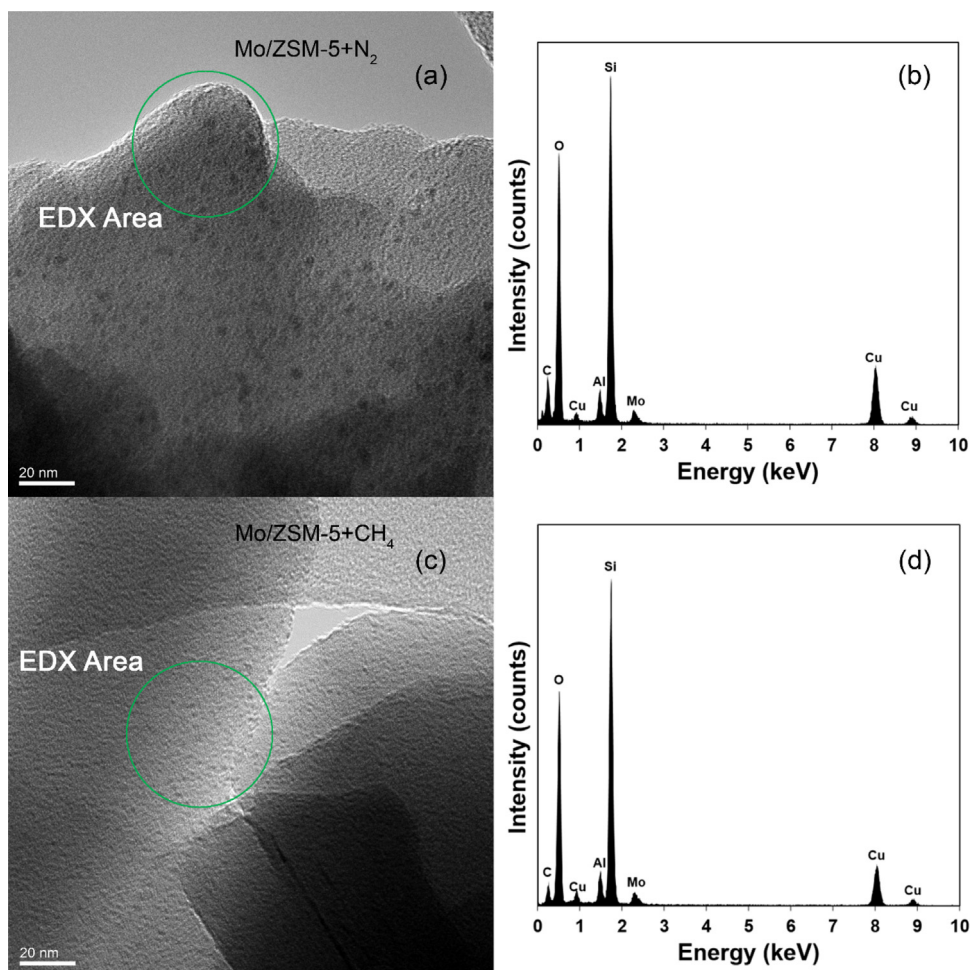
Fig. 8. TEM images and the corresponding EDX spectra of spent Mo/ZSM-5 collected after catalytic *n*-butylbenzene cracking under the environment of N_2 (a and b) and CH_4 (c and d).

performance. The catalytic active center widely reported in literature work at higher temperatures such as 700 °C is molybdenum carbide species, like Mo_2C, which is not observed on the XPS spectra of spent catalysts, suggesting that the active catalytic center might be the molybdenum oxide species, such as MoO_3 and MoO_2, in this work.

In a similar matter, O surface concentration is reduced after upgrading reaction under N_2 environment as shown in Fig. 9b. Nonetheless, surface O signal is even increased after methane run compared to that from the fresh sample, indicating more oxygen exposed to the catalyst's surface probably due to the back diffusion of Mo as mentioned above, which might be closely correlated to its better performance. Besides, the binding energy of surface O at 532.6 eV matches the characteristic one from O in SiO_2 abundant in the ZSM-5 support. The presence of surface oxygen coming from molybdenum and aluminum oxides is not observed in all three spectra included in Fig. 9b, which is probably attributed to their significantly less abundance in the catalyst and masking effect of the surface O signal from SiO_2.

C 1s signal is also monitored over the solid samples collected from various runs to trace the tendency of carbon deposition which has been identified as the main contributor to catalyst deactivation during heavy oil upgrading [48,49]. As demonstrated in Fig. 9c, carbon signal is noticed from all the samples tested to certain degree. The residue carbon observed on the surface of fresh catalyst might be due to the adsorption of CO_2 and/or other carbon containing compounds during sample storage. Coke formation is clearly wit-

nessed from the stronger peak intensity in the spectra collected over the catalyst after upgrading reaction under both N_2 and CH_4 environments. Nevertheless, lower C 1s signal at binding energy of 284.8 eV is clearly observed in the spectra from the methane run when that from its N_2 counterpart is referred, which is consistent with the coke yield results as reported in Table 1. In addition, it is also worth noting that there is an additional small peak at 288.8 eV present in the spectra collected over the spent catalyst, which might be due to the existence of residue hydrocarbons left over from the upgrading reaction on the catalyst surface.

4. Conclusions

The work reported here further demonstrates the technical feasibility of partial upgrading of bitumen with cheap methane over transition metal modified zeolite at moderate conditions to yield partially upgraded crude oil suitable for pipeline transportation with no or significantly reduced need of diluent addition. Even though it may not meet all the industrial application criteria at the current stage, the improved bitumen quality and the involvement of methane in the reaction are clearly evidenced, which shed lights on the proposed application. With methane introduction during bitumen catalytic thermal cracking, in addition to the increased productivity, the quality of the acquired oil product is also significantly enhanced in terms of flowability, density, acidity, saturation degree, heating value, distillation fractions, and compatibility under the facilitation of 5% Mo/ZSM-5. Furthermore,
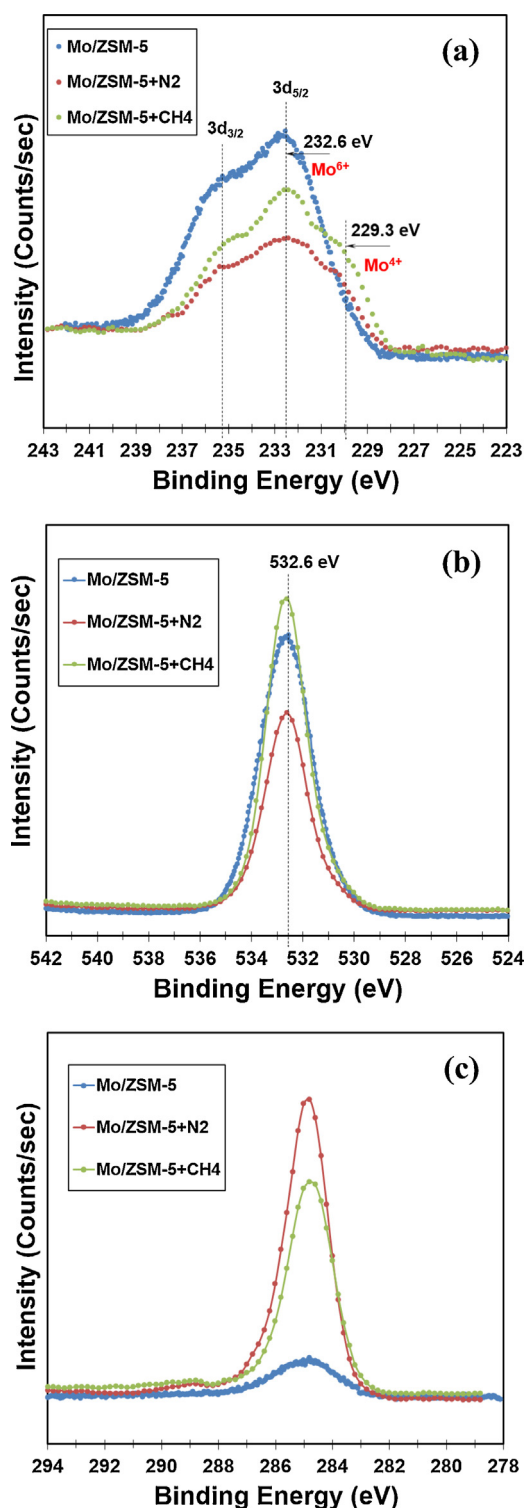
Fig. 9. XPS spectra of Mo/ZSM-5 before and after *n*-butylbenzene upgrading at 3.0 MPa and 400 °C for 20 min under different environments at (a) Mo 3d, (b) O 1s, and (c) C 1 s regions.

the methane participation into the upgrading process has been evidenced experimentally by employing well selected model compound as liquid feedstock. The ^{1}H, ^{2}D and ^{13}C NMR study of the products obtained using ^{2}D and ^{13}C enriched methane reveals that the carbon atoms from methane tend to be incorporated in the phenyl rings of the product molecules, while the hydrogen from methane favors the aromatic and benzylic sites of the product

molecules. An enhanced endothermic heat effect is also observed when methane is introduced to the upgrading reaction over the catalyst, suggesting the participation of methane in the reaction. The performance variation with feed gases, bitumen thermal cracking and catalysts apparently demonstrated the existence of synergistic effect among them. Moreover, the partially upgraded oil product can be further upgraded for gasoline and diesel productions by modifying the catalysts, which is a promising future work.

Appendix A. Supplementary data

Supplementary data associated with this article can be found, in the online version, at http://dx.doi.org/10.1016/j.apcatb.2016.08.055.

References

[1] ST-98-2016 Alberta's Energy Reserves 2015 and Supply/Demand Outlook 2016–2025, Alberta Energy Regulator, 2016.
[2] J.G. Speight, Heavy Oil Porudction Processes, Elsevier, 2013.
[3] G. Belyk, D. Burgart, B. Jablonski, J. Heida, T. Kaiser, R. Bernar, B. Whitelaw, Heavy Oil 101. Participant Handbook, Canadian Heavy Oil Association, 2013 (July).
[4] H. Topsoe, Clausen, BS, F.E. Massoth, Hydrotreating Catalysis, Springer, 1996, 2016.
[5] H. Idriss, Platin. Met. Rev. 48 (2004) 105–115.
[6] Y. Chen, A. Mahecha-Botero, C.J. Lim, J.R. Grace, J. Zhang, Y. Zhao, C. Zheng, Ind. Eng. Chem. Res. 53 (2014) 6230–6242.
[7] D. Pakhare, J. Spivey, Chem. Soc. Rev. 43 (2014) 7813–7843.
[8] P. Tang, Q. Zhu, Z. Wu, D. Ma, Energ. Environ. Sci. 7 (2014) 2580–2591.
[9] Y.G. Kolyagin, I.I. Ivanova, V.V. Ordomsky, A. Gedeon, Y.A. Pirogov, J. Phys. Chem. C 112 (2008) 20065–20069.
[10] L. Guczi, K.V. Koppány Zs Sarma, L. Borkó, I. Kiricsi, Stud. Surf. Sci. Catal. 105 (1997) 861–868.
[11] Y. Xu, L. Lin, Appl. Catal. A 188 (1999) 53–67.
[12] Y. Xu, L. Lin, J. Catal. 216 (2003) 386–395.
[13] Y. Cui, Y. Xu, J. Lu, Y. Suzuki, Z. Zhang, Appl. Catal. A Gen. 393 (2011) 348–358.
[14] M.C. Alvarez-Galvan, N. Mota, M. Ojeda, S. Rojas, R.M. Navarro, J.L.G. Fierro, Catal. Today 171 (2011) 15–23.
[15] V. Ha, A. Sarioğlan, A. Erdem-Şenatalar, Y. Taârit, J. Mol. Catal. A Chem. 378 (2013) 279–284.
[16] T.V. Choudhary, E. Aksoylu, D.W. Goodman, Catal. Rev. Sci. Eng. 45 (2003) 151–203.
[17] D. Wang, J.H. Lunsford, M.P. Rosynek, J. Catal. 169 (1997) 347–358.
[18] J. Gao, Y. Zheng, G.B. Fitzgerald, J. Joannis, Y. Tang, I.E. Wachs, S.G. Podkolzin, J. Phys. Chem. C 118 (2014) 4670–4679.
[19] Z.R. Ismagilov, E.V. Matus, L.T. Tsikoza, Energy Environ. Sci. 1 (2008) 526–541.
[20] B. Cook, D. Mousko, W. Hoelderich, R. Zennaro, Appl. Catal. A Gen. 365 (2009) 34–41.
[21] V.R. Choudhary, A.K. Kinage, T.V. Choudhary, Science 275 (1997) 1286–1288.
[22] T. Baba, H. Sawada, Phys. Chem. Chem. Phys. 4 (2002) 3919–3923.
[23] T. Baba, Y. Iwase, D. Masih, A. Matsumoto, Micro. Meso. Mater. 101 (2007) 142–147.
[24] T. Baba, K. Inazu, Chem. Lett. 35 (2006) 142–147.
[25] T. Baba, Y. Abe, Appl. Catal. A 250 (2003) 265–270.
[26] O. Anunziata, G. Mercado, L.B. Pierella, Catal. Lett. 87 (2003) 167–171.
[27] O. Anunziata, J. Cussa, A. Beltramone, Catal. Today 171 (2011) 36–42.
[28] L. Wang, Y. Xu, L. Tao, Sci. China B 40 (1997) 161–164.
[29] H. Zhang, A. Kong, Y. Ding, C. Dai, Y. Shan, J. Nat. Gas Chem. 20 (2011) 243–248.
[30] O. Anunziata, G. Mercado, L.B. Pierella, 2nd Mercosur Cong. Chem. Eng. (2005).
[31] C. Ovelles, E. Filgueiras, A. Morales, C.E. Scott, F. Gonzalez-Gimenez, B. Embaid, Fuel 82 (2003) 887–892.
[32] C. Ovelles, E. Filgueiras, A. Morales, I. Rojas, J. Jesus, I. Berrios, Energy Fuels 12 (1998) 379–385.
[33] A. Guo, C. Wu, P. He, Y. Luan, L. Zhao, W. Shan, W. Cheng, H. Song, Catal. Sci. Technol. 6 (2016) 1201–1213.
[34] P. He, H. Song, Ind. Eng. Chem. Res. 53 (2014) 15862–15870.
[35] P. He, W. Shan, Y. Xiao, H. Song, Top. Catal. 59 (2016) 86–93.
[36] Y. Xiao, P. He, W. Cheng, J. Liu, W. Shan, H. Song, Waste Manage. 49 (2016) 304–310.

[37] H. Tsaprailis, Properties of Dilbit and Conventional Crude Oils, Alberta Innovates, 2014.
[38] M.R. Gray, Upgrading Oilsands Bitumen and Heavy Oil, The University of Alberta Press, 2015.
[39] J.G. Speight, The Chemistry and Technology of Petroleum, CRC Press, 2014.
[40] P.E. Savage, D.J. Korotney, Ind. Eng. Chem. Res. 29 (1990) 499–502.
[41] P.E. Savage, M.T. Klein, Ind. Eng. Chem. Res. 26 (1987) 488–494.
[42] X. Guo, G. Fang, G. Li, H. Ma, H. Fan, L. Yu, C. Ma, X. Wu, D. Deng, M. Wei, D. Tan, R. Si, S. Zhang, J. Li, L. Sun, Z. Tang, X. Pan, X. Bao, Science 344 (2014) 616–619.
[43] V.R. Choudhary, K.C. Mondal, S.A.R. Mulla, Angew. Chem. Int. Ed. 44 (2005) 4381–4385.
[44] L. Wang, L. Tao, M. Xie, G. Xu, J. Huang, Y. Xu, Catal. Lett. 21 (1993) 35–41.

[45] B.M. Weckhuysen, D. Wang, M.P. Rosynek, J.H. Lunsford, J. Catal. 175 (1998) 338–351.
[46] R.W. Borry, Y.H. Kim, A. Huffsmith, J.A. Reimer, E. Iglesia, J. Phys. Chem. B 103 (1999) 5787–5796.
[47] E. Pretsch, P. Buhlmann, M. Badertscher, Structure Determination of Organic Compounds Tables of Spectra Data, fourth, revised and enlarged edition, Springer, 2009.
[48] M. Absi-Halabi, A. Stanislaus, Appl. Catal. 72 (1991) 193–215.
[49] M.S. Rana, V. Sámano, J. Ancheyta, J.A.I. Diaz, Fuel 86 (2007) 1231–1261.